The pulse duration has increased to 1 ns. This broadening can be attributed to the laser amplifier and drive conditions.

The DFB was then intensity modulated by the digital video multiplex shown in Fig. 5. The corresponding gated output from the 2·2 GHz receiver, produced as a single channel 'eye' pattern at the centre of the photograph, plus unwanted channels at either side, is shown in Fig. 6. The bias currents of both the laser and the amplifier, the monochromator wavelength and the polarisation state were adjusted to give the optimum ratio of gated signal to unwanted channels.

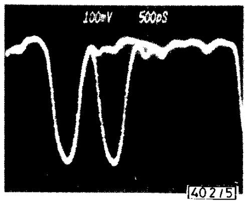

Fig. 5 *Input multiplexes*

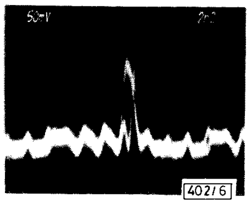

Fig. 6 *Gated video channel*

Fig. 7 shows the resultant 'eye' pattern when the receiver bandwidth was reduced to 56 MHz, which is slightly more than sufficient for a baseband channel. The gated channels were expanded to a half-amplitude width of 7 ns, and represented an inverted RZ signal which was detected by the electronic sampler and delay-lock loop, and displayed on a TV monitor.

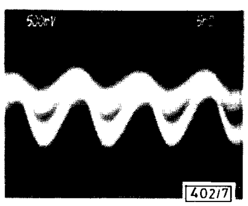

Fig. 7 *Gated video channel*
Receiver bandwidth = 56 MHz

A second DFB, modulated in turn by synchronous and asynchronous signals, was added to the system. With the monochromator set to approximately 0·5 nm resolution, either of the wavelengths could be selected while gating the amplifier. The crosstalk between wavelengths was approximately 10%, without noticeable degradation in the picture quality.

Conclusion: This experiment has shown that it is possible to use a gated laser amplifier as a means of reducing the receiver bandwidth requirement in a point-to-multipoint TV distribution system, to synchronise the sampling pulses to a channel using a delay-lock loop and to select channels by wavelength tuning. At rates up to 1·1 Gbit/s the power budget is limited by the signal-related noise of the distributed amplifier. At higher rates the performance is further limited by the restricted modulation bandwidth of the amplifier. Nevertheless, optical sampling in cable TV systems provides an alternative to electronic sampling which, if developed, should give access to more channels or improved power budgets.

Acknowledgment: We thank the Director of Research, British Telecommunications for permission to publish this letter.

D. W. FAULKNER
D. M. RUSS
J. C. REGNAULT
A. LORD

British Telecom Research Laboratories
Martlesham Heath, Ipswich IP5 7RE, United Kingdom

6th September 1988

References

1 FAULKNER, D. W., RUSS, D. M., DOUGLAS, D., and SMITH, P. J.: 'Novel sampling technique for digital video demultiplexing, descrambling and channel selection', *Electron. Lett.*, 1988, **24**, pp. 654–656
2 NELSON, A. W., DEVLIN, W. J., HOBBS, R. E., LENTON, C. G. D., and WONG, S.: 'High-power, low-threshold BH lasers operating at 1·52 μm grown entirely by MOVPE', *ibid.*, 1985, **21**, pp. 888–889
3 IKEDA, M.: 'Switching characteristics of laser diode switch', *IEEE J. Quantum Electron.*, 1983, **QE-19**, pp. 157–164
4 YAMAMOTO, Y.: 'Noise and error rate performance of semiconductor laser amplifiers in PCM-IM optical transmission systems', *ibid.*, 1980, **QE-16**, pp. 1073–1081

CONTINUOUSLY TUNABLE 1·5 μm MULTIPLE-QUANTUM-WELL GaInAs/GaInAsP DISTRIBUTED-BRAGG-REFLECTOR LASERS

Indexing term: Semiconductor lasers

We demonstrate improved performance in tunable distributed-Bragg-reflector lasers using GaInAs/GaInAsP multiple-quantum-well active layers. We observe linewidths as low as 1·9 MHz, differential quantum efficiencies as large as 33%/front facet at 1·5 μm, and rapid electronic access to all frequencies throughout a 1000 GHz range.

Tunable narrow-linewidth semiconductor lasers can be expected to play a major role in future lightwave systems, both in high-capacity point-to-point links as well as in networking and switching applications. In this letter we describe improved performance in tunable lasers using GaInAs/GaInAsP multiple-quantum-well (MQW) active layers and thin etch-stop layers for reproducible fabrication techniques.

Fig. 1 shows the basic three-section, three-electrode, distributed Bragg reflector (DBR) laser design,[1,2] where we have

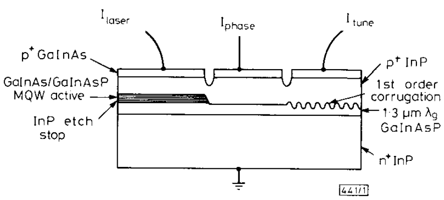

Fig. 1 *Longitudinal structure of three-section continuously tunable MQW-DBR laser*

employed MQW active layers.[3] The detailed sequence in the gain section is an n^+ InP substrate with an n^+ InP buffer, ~2500 Å of n-type 1·3 μm λ_{PL} (photoluminescence wavelength) Q (quaternary GaInAsP) serving as the majority of the waveguide core, a 250 Å n-type InP etch-stop layer, four sequences of 100 Å 1·3 λ_{PL} Q barriers and 80 Å GaInAs quantum wells, ~500 Å p^- 1·3 λ_{PL} Q, and an upper 1·5 μm-thick p^+ InP cladding with a ~0·5 μm p^+ GaInAs cap. The lateral structure is the previously described[4] semi-insulating planar buried heterostructure geometry, and all epitaxy is done with atmospheric-pressure MOCVD. No optical coatings were applied to any of the devices studied here.

Fig. 2 shows typical TE and TM optical spectra of at $0{\cdot}9 I_{th}$ for devices with gain, phase and Bragg section lengths of $400\,\mu m$, $60\,\mu m$ and $350\,\mu m$, respectively, and $20\,\mu m$ isolation

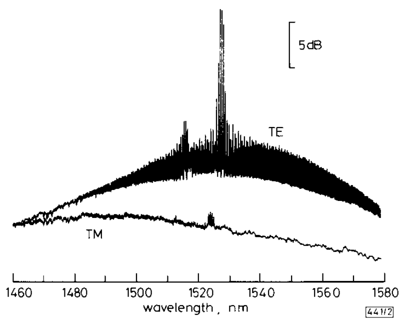

Fig. 2 *Below threshold logarithmic scale spectrum of TE and TM emission* ($I = 0{\cdot}9 I_{th}$)

grooves between the sections. Well outside the Bragg band the finely spaced Fabry–Perot modes of the entire cavity evident in the TE emission have negligible ripple, indicating that the structure achieves the high level of optical continuity essential for reproducible, well behaved tuning characteristics. Side mode suppression above threshold can be as high as 45 dB, and easily exceeds 30 dB unless the Bragg or phase current is adjusted to be very near a mode transition. The TM emission is highly suppressed with its peak shifted to higher energy. This results from the reduced matrix element[5] between the conduction band and the heavy-hole valence band near $k_{\parallel} = 0$. For direct modulation, this will drastically reduce any potential TM mode-partition problems.

The excellent optical continuity along the guide is also confirmed by the light/current (L/I) characteristics. Fig. 3 shows the CW 23°C L/I curve for the device shown in Fig. 2, with

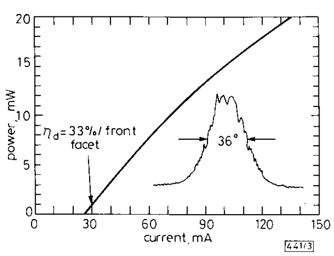

Fig. 3 *CW light/current characteristic at 23°C of three-section MQW-DBR*

Inset shows stable far field

the phase section open-circuited and the Bragg section shorted through a $50\,\Omega$ resistance. The differential quantum efficiency η_d at low power is 33%/front facet, indicating very low cavity loss. Output power exceeds 20 mW with no mode hop in this device; the inset shows the stable 36° FWHM far field. The maximum power and η_d probably can be improved further with optimised output facet coatings.

Linewidths which saturated at a minimum value of ~3–4 MHz were achievable in most devices measured. Fig. 4 shows the best device, with a minimum linewidth of 1·9 MHz as seen in the delayed self-heterodyne beat spectrum shown in the inset. The linewidth is plotted both against power and inverse power, and the linewidth-power product of 7 MHz mW is very low for a single-cavity semiconductor laser.

Fig. 5 shows a typical tuning characteristic for these devices. The lower set of curves shows the phase-section current required to achieve the operating wavelength read along the abscissa for each of the 13 selectable longitudinal modes of the structure. Across the entire range the Bragg currents run from −1 mA to ~90 mA. Each curve has a different initial Bragg current for mode selection, but in addition the Bragg current is varied with the phase current a small amount along each curve to maximise the total sweep range of each mode. For

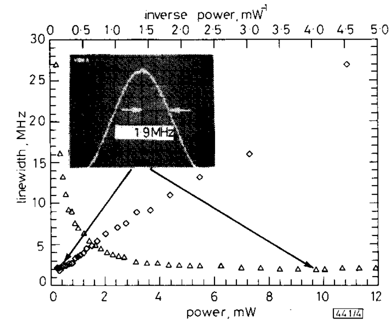

Fig. 4 *CW linewidth against power* (Δ) *and inverse power* (◇) *as measured by delayed self-heterodyne technique*

Inset shows beat spectrum, revealing 1·9 MHz laser linewidth

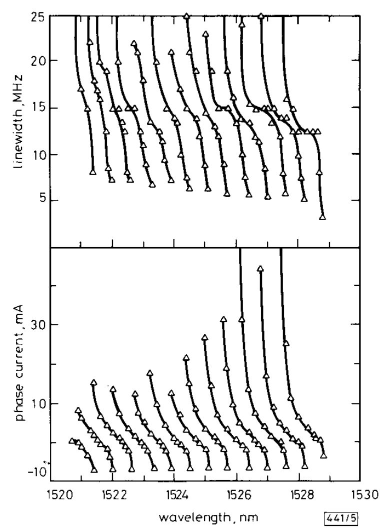

Fig. 5 *Tuning characteristics of three-section MQW-DBR*

Bottom shows phase current required to achieve a specified wavelength for each of 13 different Bragg-selectable modes. Bragg current is also varied slightly along each trace to maximise sweep range of each mode. Upper curves show CW linewidth for each mode as tuning occurs. Entire 1000 GHz range can be spanned while keeping linewidth below ~16 MHz

the short ($60\,\mu m$) phase section device shown here, the total tuning range exceeds 1000 GHz (~80 Å) and the sweep range is ~150 GHz (~14 Å). This exceeds the ~6 Å free spectral range by more than a factor of two, thus easily providing a guarantee of continuous electronic accessibility of any wavelength throughout the 1000 GHz range. This continuous sweeping range can usually be accomplished with only one current variation and a linear resistive current divider.[1] Longer (~$234\,\mu m$) phase section devices had similar characteristics with a slight reduction in η_d, but offered a larger local sweep of 250 GHz (~21 Å).

The upper part of Fig. 5 shows the linewidth behaviour as the device is tuned. Provided one only scans an amount sufficient to achieve complete electronic coverage (one free spectral range), linewidths can always be maintained below ~16 MHz across the entire 1000 GHz tuning range. Reduced linewidth results from both the high-Q cavity and the reduced linewidth enhancement factor α in the quantum-well gain medium. The latter was determined to have a value of $\sim -4{\cdot}5$ by monitoring simultaneously the FM sideband spectrum and the IM waveform under high speed direct modulation.[6]

These devices are suitable for both high-quality tunable local oscillators or medium-bit-rate FSK transmitters. Flat FM response can be obtained up to the $\sim$100 MHz limit imposed by the free carrier lifetime, with the large response ($\sim$10–15 GHz/mA) evident in Fig. 5 overpowering any thermal effects at low frequencies. Direct modulation is also possible, but any speed benefits resulting from increased quantum-well differential gain are overshadowed by the longer photon lifetime and reduced photon density due to the placement of the quantum wells with respect to the waveguide core. Linear variation of the relaxation oscillation frequency f_{RO} against $P^{1/2}$ was observed, but even at powers of 18 mW, f_{RO} had only achieved $\sim$6 GHz. The devices do exhibit low chirp (1·8 Å 20 dB down) under 5 Gbit/s direct modulation with a 3 : 1 extinction ratio; at higher extinctions the high-Q-enhanced relaxation oscillations induce pattern effects and eye closure. A high extinction would probably be possible with a front facet coating.

In closing, we have demonstrated improved performance in continuously tunable semiconductor lasers using quantum-well active layers and ultrathin etch-stop fabrication techniques. These lasers offer reproducible spectral properties, and look promising for practical coherent technology.

T. L. KOCH
U. KOREN
R. P. GNALL
C. A. BURRUS*
B. I. MILLER

AT&T Bell Laboratories
**Crawford Hill Laboratory*
Holmdel, NJ 07733, USA

19th September 1988

References

1 MURATA, S., MITO, I., and KOBAYASHI, K.: 'Over 720 GHz (5·8 nm) frequency tuning by a 1·5 μm DBR laser with phase and Bragg wavelength control regions', *Electron. Lett.*, 1987, **23**, pp. 403–405
2 KOTAKI, Y., MATSUDA, M., YANO, M., ISHIKAWA, H., and IMAI, H.: '1·55 μm wavelength tunable FBH-DBR laser', *ibid.*, 1987, **23**, pp. 325–327
3 KOREN, U., MILLER, B. I., SU, Y. K., KOCH, T. L., and BOWERS, J. E.: 'Low-internal-loss separate confinement heterostructure InGaAs/InGaAsP quantum well laser', *Appl. Phys. Lett.*, 1987, **51**, p. 1744
4 KOREN, U., MILLER, B. I., EISENSTEIN, G., TUCKER, R. S., RAYBON, G., and CAPIK, R. J.: 'Semi-insulating blocked planar BH GaInAsP/InP laser with high power and high modulation bandwidth', *Electron. Lett.*, 1988, **24**, pp. 138–140
5 ASADA, M., KAMEYAMA, A., and SUEMATSU, Y.: 'Gain and intervalence band absorption in quantum-well lasers', *IEEE J. Quantum Electron.*, 1984, **QE-20**, pp. 745–753
6 HARDER, C., VAHALA, K., and YARIV, A.: 'Measurement of the linewidth enhancement factor α of semiconductor lasers', *Appl. Phys. Lett.*, 1983, **42**, p. 328

THE SSFIP: A GLOBAL CONCEPT FOR HIGH-PERFORMANCE BROADBAND PLANAR ANTENNAS

Indexing terms: Antennas, Planar antennas, Microstrip

The SSFIP (strip–slot–foam–inverted patch) antenna presents significant advantages over standard microstrip antennas: very broad bandwidth, high efficiency, low crosspolarisation level, integrated radome, lightweight and rigid construction and low cost. A 16-element array with more than 16 dB gain and 21·1% bandwidth for SWR ≤ 2 shows what can be achieved.

Introduction: Microstrip patch antennas present significant advantages in terms of size, ease of fabrication and compatibility with printed circuits, but also a number of drawbacks, ranging from narrow bandwidth to low efficiency. Surface waves produce diffraction at the dielectric's edges and coupling between array elements, contributing to higher sidelobes and crosspolarisation levels. The use of a single substrate for both the radiating elements and the feed network is a poor compromise, since two contradictory functions are expected from the same structure. These problems and others were discussed recently by Hall *et al.*[1] Last but not least, patch antennas should be protected by a cover against environmental effects.

Taking all these factors into consideration a new global concept, the strip–slot–foam–inverted patch antenna, has been developed. Low-cost materials are used, the substrate being a low loss, low-permittivity foam to prevent surface wave propagation and to increase the bandwidth. The radiating patches are deposited on the underside of a thin plastic sheet (standard epoxy fibre-glass substrate), that also serves as protective cover. They are fed via wide coupling slots by a microstrip line located on a high-quality dielectric substrate underneath the ground plane (Fig. 1).

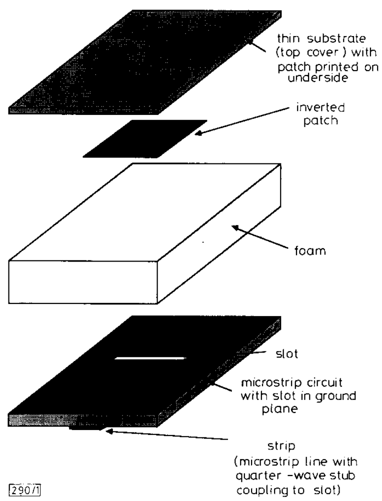

Fig. 1 *Exploded view of SSFIP antenna structure*

16-element SSFIP array with 21·1% bandwidth: A single-element antenna was first realised with the following materials:

(*a*) Microstrip substrate: RT/Duroïd 5870, $\varepsilon = 2{\cdot}33$, $h = 0{\cdot}254$ mm, with a 100 Ω microstrip line exciting a slot in the ground plane.

(*b*) Foam: polymethacrylamid hard foam, $\varepsilon = 1{\cdot}07$, $\tan\delta = 8 \times 10^{-4}$, $h = 2$ mm.

(*c*) Patch support: epoxy fibre-glass, $\varepsilon = 4{\cdot}32$, $h = 0{\cdot}1$ mm, patch on underside.

The relative bandwidth of the final design, determined by experiment, was 11·7% for a SWR ≤ 2. The measured maximum gain was 5·8 dB.

Using the optimised dimensions of this single-element antenna, a 16-element broadside antenna array (4 × 4) with a corporate feed network was designed. The feed network was carefully designed to reduce as well as possible the frequency sensitivity. The CAD/CAM program MICROS 6[2] was used to design and realise this array. Fig. 2*a* shows the mask of the feed network and Fig. 2*b* one of the slot array, both etched on an RT/Duroïd substrate (after aligning the masks). The mask of the 16 square patches, spaced 0·66 λ apart, is shown in Fig. 2*c*.